A New Alternating Ferro- and Antiferromagnetic, One-Dimensional Manganese(II) Azide Complex, $[Mn(dpa)(N_3)_2]$ − Crystal Structure and Spectroscopic and Magnetic Properties

Mónica Villanueva,[a] José L. Mesa,[a] Miren K. Urtiaga,[a] Roberto Cortés,[b] Luis Lezama,[a] María I. Arriortua,[a] and Teófilo Rojo*[a]

Keywords: Coordination chemistry / EPR spectroscopy / Magnetic properties

The synthesis, crystal structure, and spectroscopic and magnetic properties of a new alternating ferro- and antiferromagnetic, one-dimensional manganese(II) azide complex, $[Mn(dpa)(N_3)_2]$ (where dpa is the 2,2′-dipyridylamine ligand), are reported. The compound's crystal structure has been resolved at room temperature. The complex crystallizes in the monoclinic $P2_1/c$ space group, with a = 7.089(2), b = 19.090(4), and c = 9.682(4) Å, β = 104.61(2) °, and Z = 4. The structure consists of neutral chains in which each Mn^{II} cation is alternatively bridged by two end-on and two end-to-end azido bridges. The octahedral coordination of the metallic cation is completed by two dpa ligand nitrogen atoms. Reflectance measurements confirm the hexacoordination of the Mn^{II} ions in the complex. The ESR spectra at room temperature and at 4.2 K are isotropic, with a mean g-value of 2.010(1). Magnetic data were analyzed on the basis of an alternating ferro- and antiferromagnetic Heisenberg chain of Mn^{II} ions. The J-exchange parameters found are 64.3 and –75.7 K. A spin canting phenomenon has been observed in this compound, with a remnant magnetization which vanishes above 15 K. Magnetostructural correlations in manganese(II) systems of alternating magnetic sign are discussed.

Introduction

The synthesis and characterization of new low-dimensional materials (one or two-dimensional) that may show ferromagnetic long-range cooperative phenomena (molecular magnets)[1−6] have in recent years been the main focus of interest in the molecular magnetism area. At present, the field of molecular magnetism is addressing the synthesis and study of discrete polynuclear molecules in an attempt to improve our understanding of the mechanism involved in magnetic coupling[7,8] and the production of new paramagnetic clusters with high spin and strong anisotropy (superparamagnetic molecules).[9,10]

The azide-pseudohalide anion is an excellent ligand for obtaining one-dimensional,[11,12] two-dimensional,[13] or three-dimensional[14] polynuclear systems with divalent metal ions. From the magnetic point of view, the most interesting characteristic of azido-bridged complexes is that the azido ligand can act as a very effective superexchange pathway, due to the different coordination modes. Normally, the end-to-end (EE) bridge produces antiferromagnetic coupling, whereas the end-on (EO) form gives ferromagnetic coupling. Both the EE and EO structural bridges may coexist within the same (one- or two-dimensional) system, owing to different distances and/or angles found in the structure. These systems are globally antiferro- or ferromagnetic, but they belong to the so-called "magnetic systems alternating in sign". In compounds of this kind, two or more exchange coupling parameters (J) are necessary to fit the experimental results, in contrast to the "uniform magnetic systems" in which all azido bridges have both the same coordination mode and the same structural parameters.

Taking the aspects mentioned above into account, this work was focused on the preparation and characterization of a new polynuclear azido complex. With this aim in mind, we used the bidentate ligand 2,2′-dipyridylamine with a metal/bidentate ligand 1:1 ratio, in such a way that the four coordination vacancies around the six-coordinated manganese(II) ion should be completed by the excess of the azido ligands. Following this procedure, we have synthesized a new alternating ferro/antiferromagnetic, one dimensional manganese(II) azide complex, which has been characterized by X-ray diffraction and spectroscopic techniques. Magnetic measurements indicate global antiferromagnetic behavior, with the presence of a weak ferromagnetic component intrinsic to the sample.

Results and Discussion

Description of the Structure

Selected bond lengths and angles of $[Mn(dpa)(N_3)_2]$ are given in Table 1. The structure consists of linear neutral chains extending along the [100] crystallographic direction (Figure 1). The Mn^{II} ions are alternatively linked by two EO (end-on) azido bridges [Mn(1)−N(4),N(4)^{i}; 2.231(2), 2.218(2) Å] and two EE (end-to-end) ones [Mn(1)−N(7),N(9)^{ii};

[a] Departamento de Química Inorgánica and Departamento de Mineralogía-Petrología Facultad de Ciencias, Universidad del País Vasco,
Apdo. 644, 48080 Bilbao, Spain
Fax: (internat.) + 34-94/464-8500
E-mail: qiproapt@lg.ehu.es
[b] Departamento de Química Inorgánica, Facultad de Farmacia, Universidad del País Vasco,
Apdo. 450, 01080 Vitoria, Spain

  1434−1948/01/0606−1581 $ 17.50+.50/0

2.275(2), 2.274(2) Å]. The Mn^{II} ions exhibit octahedral coordination, completed by the two N(1) and N(3) nitrogen atoms of the 2,2′-dipyridylamine ligand [Mn(1)−N(1),N(3); 2.253(2), 2.243(2) Å]. The existence of an inversion center induces the Mn(1)−N(4)−Mn(1)^{i}−N(4)^{i} bridging unit to form a plane. The EO bridging azides are quasilinear [N(4)−N(5)−N(6), 178.7(3)°]. The Mn(1)−N(4)−Mn(1)^{i} angle in the EO mode is 102.92(7)°, in good agreement with the results obtained (100−105°) for this kind of bridging ligand.[15−17] For the EE bridges, the Mn(1)−N(7)−N(8) angle is 125.0 (1)° and the Mn(1)^{ii}−N(9)−N(8) angle is 127.74(2)°. The torsion angle τ between the mean plane of Mn(1)−N(7)−N(8)−N(9) and Mn(1)^{ii}−N(9)−N(8)−N(7) for a chair configuration is 64.2(2)°. The dihedral angle δ between the least-squares plane defined by the six nitrogen atoms of the EE bridging azides and the N(7)−Mn(1)−N(9)^{ii} system is 35.10(6)°. The intrachain Mn···Mn distances are 3.479(1) and 5.432(1)Å in the EO and EE bridges, respectively.

Table 1. Selected bond lengths [Å] and angles [°] for $[Mn(C_{10}H_9N_3)(N_3)_2]$, (e.s.d. in parentheses; Symmetry codes: $i = -x,-y,-z$; $ii = -x+1,-y,-z$)

Bond lengths (Å)			
Mn(1)−N(1)	2.253(2)	N(5)−N(6)	1.141(3)
Mn(1)−N(3)	2.243(2)	N(7)−N(8)	1.177(3)
Mn(1)−N(4)	2.231(2)	N(8)−N(9)	1.166(3)
Mn(1)−N(7)	2.275(2)	N(1)−C(1)	1.359(3)
Mn(1)−N(4)^{i}	2.218(2)	N(1)−C(5)	1.333(3)
Mn(1)−N(9)^{ii}	2.274(2)	N(2)−C(5)	1.378(3)
Mn(1)^{i}−N(4)	2.218(2)	N(2)−C(6)	1.378(3)
Mn(1)^{ii}−N(9)	2.274(2)	N(3)−C(6)	1.335(3)
N(4)−N(5)	1.194(3)	N(3)−C(10)	1.356(3)
Bond angles (°)			
N(3)−Mn(1)−N(4)	91.86(7)	N(3)−Mn(1)−N(4)^{i}	168.91(7)
N(3)−Mn(1)−N(7)	99.07(7)	N(4)−Mn(1)−N(7)	168.29(7)
N(3)−Mn(1)−N(1)	82.55(7)	N(8)−N(9)−Mn(1)^{ii}	127.74(2)
N(3)−Mn(1)−N(9)^{ii}	90.3(8)	N(5)−N(4)−Mn(1)^{i}	129.0(1)
N(4)^{i}−Mn(1)−N(1)	99.95(7)	Mn(1)−N(7)−N(8)	125.0(1)
N(4)^{i}−Mn(1)−N(4)	77.08(7)	Mn(1)−N(4)−N(5)	127.3(1)
N(4)^{i}−Mn(1)−N(7)	91.90(7)	Mn(1)−N(4)−Mn(1)^{i}	102.92(7)
N(4)^{i}−Mn(1)−N(9)^{ii}	88.88(8)	N(4)−N(5)−N(6)	178.7(3)
N(1)−Mn(1)−N(4)	99.87(7)	N(7)−N(8)−N(9)	178.6(2)
N(1)−Mn(1)−N(7)	85.77(7)	Mn(1)−N(1)−C(5)	127.7(1)
N(4)−Mn(1)−N(9)^{ii}	90.48(8)	C(5)−N(2)−C(6)	134.4(2)
N(7)−Mn(1)−N(9)^{ii}	85.31(8)	Mn(1)−N(3)−C(6)	127.9(1)
N(1)−Mn(1)−N(9)^{ii}	167.64(7)		

The bond lengths and angles for the 2,2′-dipyridylamine molecule are in the range usually found in this kind of molecule. This ligand may be considered as nonplanar, since the value of the dihedral angle between the pyridine rings is 5.84(8)°.

IR and UV/Visible Spectroscopy

The points of interest in the IR spectrum of the $[Mn(dpa)(N_3)_2]$ complex lie mainly in the bands due to the azido groups. The asymmetrical stretch, $\nu_{asym}(N_3)$, appears split as a strong band at ca. 2095 and 2050 cm^{-1}, in good agreement with the simultaneous existence of EO and EE bridging modes in the complex.[18] The azide symmetric stretch $\nu_{sym}(N_3)$, corresponding to the EO bridging mode, can be observed as a band of medium intensity at about 1330 cm^{-1}. This mode is not active for the symmetrical EE coordination. Finally, the band corresponding to the deformation mode of the azido group, $\delta(N_3)$, is found at ca. 610, 600 cm^{-1}, in good agreement with that observed for all polynuclear azido compounds.[18] Furthermore, the IR spectrum of the title compound features the bands characteristic of the 2,2′-dipyridylamine molecule, seen in the stretching and bending modes of the C−C and C−N bonds in the ranges between ca. 1645−1360 and 1270−750 cm^{-1}.

The diffuse reflectance spectrum of $[Mn(dpa)(N_3)_2]$ exhibits several very weak, spin-forbidden d-d bands, at ca. 17240, 21275, 22990, 25974, and 30770 cm^{-1}, as would correspond to a d^5 high spin cation of ideal octahedral symmetry.[19−21]

ESR and Magnetic Properties

ESR spectra of $[Mn(dpa)(N_3)_2]$, at room temperature and at 4.2 K, were performed on a powdered sample. The spectra are isotropic, with a g-value of 2.010(1). The linewidths are of 116.0 and 304.0 Gauss at 300 and 4.2 K, respectively.

The magnetic susceptibility of $[Mn(dpa)(N_3)_2]$ was measured, using a powdered sample, from 4.2 to 300 K at magnetic fields of 0.1 and 0.01 T. The plots of χ_m and $\chi_m T$ vs. temperature, obtained when the magnetic measurements were recorded at a magnetic field of 0.1 T, are shown in Figure 2. The magnetic susceptibility increases with decreasing temperature down to about 27 K; after that it decreases down to ca. 18 K. An abrupt increase is then observed at about 13.5 K, followed by a decrease down to 4.2 K. A plot of reciprocal molar magnetic susceptibility vs. temperature shows classical Curie-Weiss behavior above 50 K. The calculated Curie and Curie−Weiss constants are $C_m = 4.77\ cm^3$ K/mol and $\theta = -27.5$ K, respectively. The magnetic susceptibility curve obtained using a magnetic field of 0.01 T shows similar features, but the increase observed after the magnetic ordering is more abrupt than that observed at 0.1 T (see inset in Figure 2). The negative Weiss temperature, together with the decrease in the effective magnetic moment observed when the temperature is lowered (5.90 BM at 300 K and 1.46 BM at 4.2 K (see Figure 2), are indicative of the existence of antiferromagnetic exchanges as major interactions for the $[Mn(dpa)(N_3)_2]$ compound. However, the increase in susceptibility at low temperatures indicates the presence of a weak intrinsic ferromagnetic contribution, possibly due to a spin canting effect in the compound.

In order to corroborate this result and to calculate the Neel temperature, magnetization measurements were carried out. Figure 3 shows the zero-field magnetization curve vs. temperature for the compound, previously cooled in a magnetic field of 0.01 T. It can be observed that the remnant magnetization decreases with increasing temperature and vanishes above $T_N = 15$ K. This fact implies the existence of a small amount of ferromagnetic component in the ordered state, which appears to be responsible for the steep

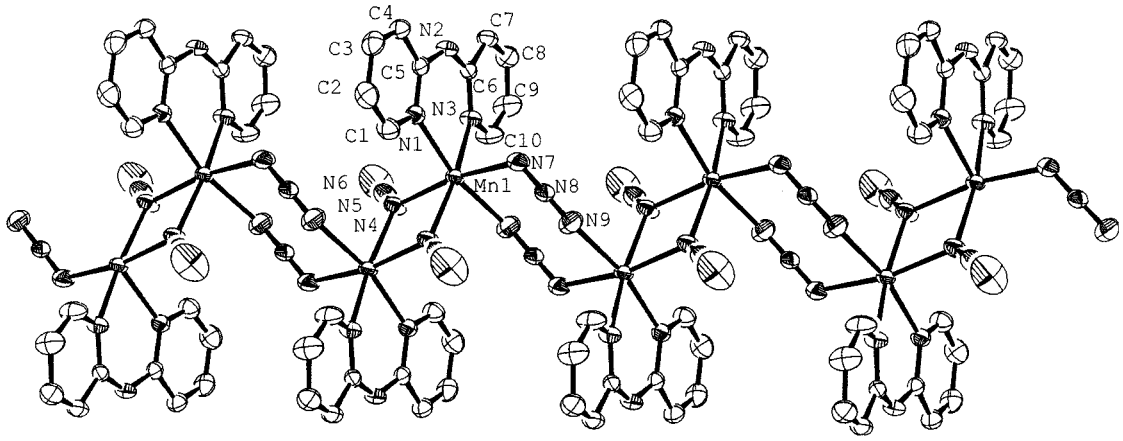

Figure 1. ORTEP drawing (50% thermal ellipsoids) of the $[Mn(dpa)(N_3)_2]$ chain complex showing the alternating end-on and end-to-end coordination of the azido ligands and atom-labeling scheme. The chain runs along the *a*-axis

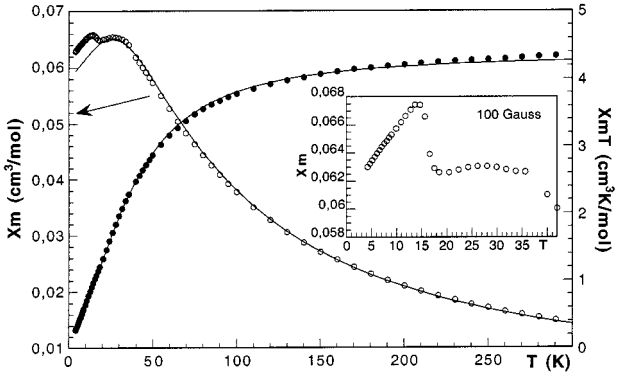

Figure 2. Thermal evolution of χ_m and χ_mT curves of $[Mn(dpa)(N_3)_2]$. The inset shows the χ_m vs. T curve at 100 Gauss. The solid lines show the fit of the χ_m and χ_mT experimental data to the model for alternating ferromagnetic-antiferromagnetic $S = {}^5/_2$ chain

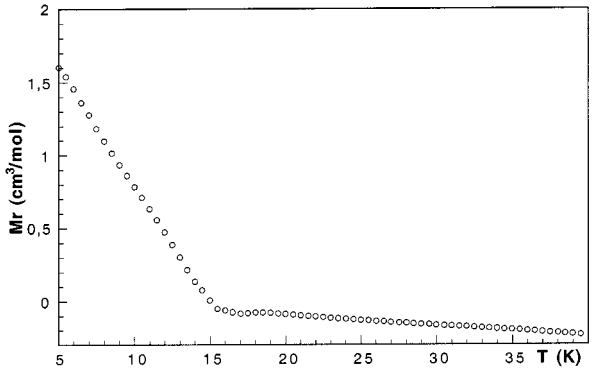

Figure 3. Remnant magnetization vs. temperature of $[Mn(dpa)(N_3)_2]$

increase observed in χ_m at temperatures lower than the ordering temperature.

The magnetic susceptibility data at 0.1 T have been interpreted on the basis of a theoretical model for the alternating ferromagnetic-antiferromagnetic $S = {}^5/_2$ chain, using the following expression for the susceptibility:[18]

$$\chi_m = [Ng^2\beta^2/3kT][1 + u_1 + u_2 + u_1u_2/1 - u_1u_2]$$

where, $u_1 = \coth(J_1/kT) - (kT/J_1)$ and $u_2 = \coth(J_2/kT) - (kT/J_2)$. In order to make a quantitative comparison with the theoretical expression deduced in the classical limit, we used the $J_i \rightarrow J_iS(S+1)$ and $g \rightarrow g[S(S+1)]^{1/2}$ scaling factors. Good agreement between the experimental magnetic data and the theoretical model was obtained when the two interactions, J_1 and J_2, had opposite signs. Fixing "*g*" to the value of 2.01 for manganese(II) ion (from the ESR spectra), the best agreement (solid lines in Figure 2) corresponds to the following parameters: $J_1 = 64.3$ K (45.3 cm^{-1}), and $J_2 = -75.7$ K (-53.3 cm^{-1}). The model used appears to provide a very good description of the susceptibility between 18 and 300 K, as the discrepancy does not exceed the experimental uncertainty. At very low temperature, the agreement is less satisfactory, due probably to the influence of small interchain interactions and the weak ferromagnetic contribution present in this compound.

Magnetostructural Correlations

It is possible to carry out a study concerning magnetostructural correlations in compounds with alternating double EO and EE azido bridges, as several complexes of this kind have recently been reported (Table 2).

The main factor controlling the intensity of the exchange ferromagnetic interactions in the EO bridge appears to be the bridging angle. Here, the larger the bridging angle is, the larger are the ferromagnetic interactions. For EE bridges, however, more structural parameters have recently been studied: namely δ [dihedral angle between the plane defined for the six N-azido atoms and the N(1)−Mn−N(3′) plane] and τ [angle between the mean planes Mn−N(1)−N(2)−N(3) and N(1)−N(2)−N(3)−Mn′]. For the d^5 EE azido-bridged compounds, the most useful parameter is the dihedral angle (δ).

In order to analyze the magnetostructural correlations between δ, τ, and the superexchange *J* parameter, the Hay−Thibeault−Hoffmann[22] relationship between $\Sigma\Delta^2$ and the antiferromagnetic component of *J* is useful. The Δ values (difference in energy between MOs, derived from magnetic orbitals, of the same symmetry) may easily be ob-

Table 2. Magnetostructural Parameters for Several Related Azide 1D-Complexes

Compound	M−N−M (deg)	M...M (Å) EO	M...M (Å) EE	M−N−N (deg)	τ (deg)	δ (deg)	J (cm^{-1}) EE	J (cm^{-1}) EO	α	ref.
$[Mn(bipy)(N_3)_2]_n$	101.0	3.455	5.343	131.1 127.3	41.1	22.7	−11.9	10.0	1.2	18
$[Mn(bpm)(N_3)_2]_n$	102.9	3.496	5.484	129.1 134.2	41.1	20.5	−63.7	15.7	4.2	24
$[Mn(3\text{-}Bzpy)_2(N_3)_2]_n$	100.4	3.416	5.229	126.0 126.1		26.6	−12.3	3.5	3.5	25
$[Mn(dpa)(N_3)_2]_n$	102.9	3.479	5.432	125.0 127.7	64.2	35.1	−53	45	1.2	this work
$[Mn(3\text{-}Et,4\text{-}Mepy)_2(N_3)_2]_n$	99.7	3.402	5.149	124.8 123.2	51.2	31.7	−13.7	2.4	5.7	26
			EE	bridges only						
$[Mn(3\text{-}Etpy)_2(N_3)_2]_n$			5.418	134.7 131.7	13.5	6.9	−11.7	−		27
			5.463	134.8 129.7	23.2	11.6	−13.8	−		
$[Mn(pyOH)_2(N_3)_2]_n$				123.8 122.4	63.1	38.0	−7.0	−		27

tained by means of MO extended Hückel (EHMO) calculations. The CACAO [23] program was used on a modeled fragment possessing double EE bridges − $[(NH_3)_4Mn(NNN)_2-Mn(NH_3)_4]$ (Scheme 1) − varying the δ and τ parameters inside the limits δ = 0°/60° (this range is used because larger angles seem to be sterically hindered) and equivalent τ = 0°/95°. The manganese(II) ions were positioned in a slightly distorted octahedral environment. The N−Mn−N angle was taken as 90°, and the Mn−N(NH_3) and Mn−N(azide) bond lengths were 2.15 and 2.20 Å, respectively, as observed from the structural data. The atomic parameters used for Mn, N, and H were the program standards.

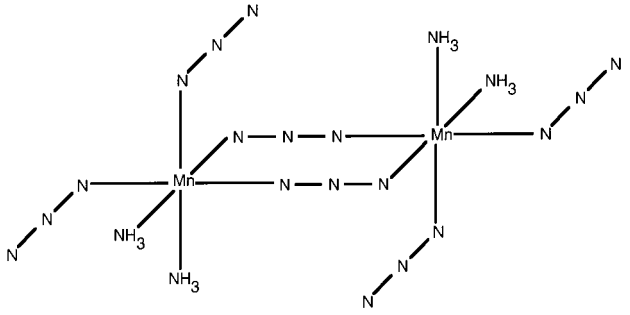

Scheme 1

Ten molecular orbitals are generated from the five magnetic orbitals, with one electron each, corresponding to the two Mn^{II} ions. The antiferromagnetic contribution should be proportional to the sum: $\Sigma\Delta^2 = \Delta^2(d_{x^2-y^2}) + \Delta^2(d_{z^2}) + \Delta^2(d_{xz}) + \Delta^2(d_{xy}) + \Delta^2(d_{yz})$. However, priority was given in each modeled system to the orbitals mainly implicated in the exchange pathway. The results of the calculations were plotted as $\Sigma\Delta^2$ vs. δ or τ (Figure 4). In the light of these data, we can deduce that the antiferromagnetic coupling should decrease for larger δ values, indicating that the loss of overlap due to the increase in the torsion angles becomes the driving parameter controlling the magnitude of the antiferromagnetic coupling.

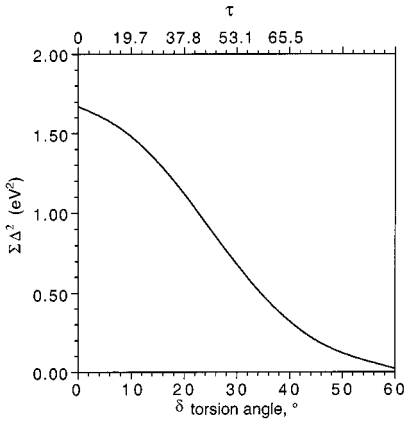

Figure 4. Evolution of the $\Sigma\Delta^2$ parameter vs. δ and τ angles

Several conclusions can be drawn from the magnetostructural parameters of the complexes, shown in Table 2. With respect to the EO bridges, it can be observed that the experimentally determined ferromagnetic J values increase with increasing bridging angle. This demonstrates the general validity of the proposed dependence of the experimental J value on α (the $|J_{EE}/J_{EO}|$ ratio) for this kind of bridging. In the case of the EE bridges, there seems to be a general tendency that the larger the torsion (δ) is, the lower

the antiferromagnetic interactions are. However, the title compound does not follow this general tendency and shows one of the largest antiferromagnetic interactions found experimentally for these alternating chains. For this kind of bridging, other factors may influence the magnitude of the antiferromagnetic exchange component. In fact, low values of Mn−N−N bridging angles have been shown to increase the antiferromagnetic interaction. In this sense, this may be the explanation for the larger J_{AF} value found in the $[Mn(dpa)(N_3)_2]$ compound, as it shows a smaller average bridging angle.

Conclusions

A new alternating ferro/antiferromagnetic, one-dimensional manganese(II) azide complex, $[Mn(dpa)(N_3)_2]$, has been synthesized and the crystal structure solved from single-crystal X-ray diffraction data. The complex exhibits a chain structure, extending along the *a*-axis with the azide anions simultaneously coordinated to the manganese(II) ions in both the end-on and the end-to-end modes. The weak bands observed in the diffuse reflectance spectrum are characteristic of the existence of manganese(II) ions in approximately octahedral environments. Isotropic signals are observed in the ESR spectra, with a mean *g*-value of 2.010(1). The linewidths of the spectra increase with decreasing temperature, probably due to the dipolar homogeneous broadening and a strong spin correlation. Magnetic measurements indicate the existence of a dominant antiferromagnetic coupling. The magnetic data have been analyzed on the basis of a model for alternating ferro- and antiferromagnetic chains of $S = 5.2$, the obtained values for the *J*-exchange parameters being of 64.3 and −75.7 K. Furthermore, the complex displays magnetization at low magnetic fields, probably due to the presence of a weak ferromagnetic component. From the magnetostructural correlations, it was possible to explain the high value obtained for the J_{AF} parameter in the $[Mn(dpa)(N_3)_2]$ complex on the basis of the low observed value of the Mn−N−N bridge angle in this compound.

Experimental Section

Syntheses: $[Mn(dpa)(N_3)_2]$ was synthesized from $Mn(NO_3)_2{\cdot}4H_2O$ (0.110 g, 0.438 mmol), 2,2′-dipyridylamine (0.075 g, 0.438 mmol), and NaN_3 (0.142 g, 2.190 mmol) in a water-methanol solution (1:1). The resulting light yellow solution was filtered off and left to stand at room temperature. After several days, prismatic, light pink, single crystals were obtained. They were separated by filtration, washed with diethyl ether, and dried over P_2O_5 for 1 h. Yield: ca. 80%. The results of CHN elemental analysis and the ICP-AES (inductively coupled plasma atomic emission spectroscopy) technique were: found C 38.4, H 2.7, N 40.3, Mn 17.5; calcd. for $C_{10}H_9MnN_9$ (310.2): C 38.7, H 2.9, N 40.6, Mn 17.7%. The density, measured by the flotation method in a mixture of $CHBr_3/CCl_4$, was 1.63(1) gcm^{-3}.

Crystal Structure Determination: A suitable single crystal of $[Mn(dpa)(N_3)_2]$ was carefully selected under a polarizing microscope and mounted on a glass fiber. Diffraction data were collected at room temperature on an Enraf−Nonius CAD4 automated diffractometer, using graphite-monochromated Mo-K_α radiation. Details of crystal data, intensity collection, and some features of the structure refinement are reported in Table 3. Lattice constants were obtained by a least-squares refinement of the setting angles of 25 reflections in the range $6° < \theta < 11°$. Intensities and angular positions of two standard reflections were measured each hour, and these showed neither decrease nor misalignment during data collection.

Table 3. Crystal data, details of data collection, and structure refinement for $[Mn(C_{10}H_9N_3)(N_3)_2]$

Formula	$C_{10}H_9MnN_9$
Molecular mass [$g{\cdot}mol^{-1}$]	310.2
Formula	$C_{10}H_9MnN_9$
Crystal system	Monoclinic
Space group	$P2_1/c$ (no. 14)
a [Å]	7.089(2)
b [Å]	19.090(4)
c [Å]	9.682(4)
β [°]	104.61(2)
V [$Å^3$]	1267.9(7)
Z	4
$\rho_{calcd.}$ [gcm^{-3}]	1.625
F(000)	628
T [K]	293(2)
μ(Mo-*Kα*) [mm^{-1}]	1.046
Radiation, λ(Mo-*Kα*) [Å]	0.71070
Limiting indices	$0<h<9$, $0<k<26$, $-13<l<13$
R [$I > 2\sigma(I)$]	$R1 = 0.039$, $wR2 = 0.096$[a]
Goodness of fit on F^2	1.065

[a] $R1 = [\Sigma(|F_o| - |F_c|)]/\Sigma|F_o|$; $wR2 = [\Sigma[w(|F_o|^2 - |F_c|^2)^2]/\Sigma[w(|F_o|^2)^2]]^{1/2}$; $w = 1/[\sigma^2|F_o|^2 + (x\,p)^2]$; where $p = [|F_o|^2 + 2|F_c|^2]/3$; $x = 0.0605$.

3944 reflections were measured, in the range $2.1° \le \theta \le 30.0°$. A total of 2664 were independent, applying the criterion $I > 2\sigma(I)$. Correction for Lorentz and polarization effects, and also for absorption with the empirical ψ scan method,[28] was performed by using the XRAYACS program.[29] Direct methods (SHELXS 97)[30] were employed to solve the structure. The metal ion was located first. The nitrogen and carbon atoms were found in difference Fourier maps. The structure was refined by the full-matrix, least-squares method based on F^2, using the SHELXL 97 computer program.[31] The scattering factors were taken from ref.[32] All non-hydrogen atoms were assigned anisotropic thermal parameters. The coordinates of the hydrogen atoms of the 2,2′-dipyridylamine ligand were obtained from difference Fourier maps. The final R factors were $R1 = 0.039$ [$wR2 = 0.096$]. Maximum and minimum peaks in final difference synthesis were 0.488, −0.397 $eÅ^{-3}$. The atomic coordinates and structure factors have been deposited at the Cambridge Crystallographic Data Centre (CCDC 146293). Drawing was made using ORTEP.[33]

Physical Measurements: CHN elemental analysis was carried out with a Perkin−Elmer Model 240 automatic analyzer. ICP-AES analysis was performed with an ARL Fisons 3410 spectrometer. The IR spectrum (KBr pellet) was obtained with a Nicolet FT-IR 740 spectrophotometer in the 400−4000 cm^{-1} range. The diffuse reflectance spectrum was recorded at room temperature on a Cary 2415 spectrometer in the 5000−47500 cm^{-1} range. A Bruker ESP

300 spectrometer was used to record the ESR polycrystalline spectra at room temperature and at 4.2 K. The temperature was stabilized by an Oxford Instrument (ITC 4) regulator. The magnetic field was measured with a Bruker BNM 200 gaussmeter and the frequency inside the cavity was determined using a Hewlett−Packard 5352B microwave frequency counter. Magnetic measurements of powdered sample were performed in the temperature range 4.2−300 K, using a Quantum Design MPMS-7 SQUID magnetometer. The magnetic field was approximately 0.1 T, a value in the range of linear dependence of magnetization vs. magnetic field even at 4.2 K.

Acknowledgments

This work was financially supported by the Universidad del País Vasco/Euskal Herriko Unibertsitatea (Project UPV 130.310-EB201/98), the Gobierno Vasco/Eusko Jaurlaritza (Project PI96/39) and the Ministerio de Educación y Cultura (Project PB97-0637), which we gratefully acknowledge.

[1] D. W. Bruce, D. O'Hare (Eds.), *Inorganic Materials*, Wiley **1992**.
[2] P. Delhaes, M. Drillon (Eds.), *Organic and Inorganic Low-Dimensional Materials*, NATO ASI Series, Vol. 168, Plenum Press, NY **1987**.
[3] D. Gatteschi, O. Kahn, J. S. Miller, F. Palacio (Eds.), *Magnetic Molecular Materials*, NATO ASI Series, Vol. 198. Kluwert, Dordrecht **1993**.
[4] E. Coronado, P. Delhaes, D. Gatteschi, J. S. Miller (Eds.), *Molecular Magnetism: from Molecular Assemblies to Devices*, NATO ASI Series, Vol. 321, Kluwer, Dordrecht **1995**.
[5] C. J. O'Connor (Ed.), *Research Frontiers in Magnetochemistry*, World Scientific, Singapore **1993**.
[6] J. Ribas, A. Escuer, M. Monfort, R. Vicente, R. Cortes, L. Lezama, T. Rojo, *Coord. Chem. Rev.* **1999**, *193−195*, 1027.
[7] R. D. Willet, D. Gatteschi, O. Kahn (Eds.), *Magneto-Structural Correlations in Exchange Coupled Systems*, NATO ASI Series, Reidel, Dordrecht **1985**.
[8] O. Kahn, *Molecular Magnetism*, VCH Publishers, Weinheim **1993**.
[9] M. M. Turnbull, T. Sugimoto, L. K. Thompson (Eds.), *Molecular-Based Magnetic Materials: Theory, Techniques and Applications*, ACS Symposium Series, n. 644, ACS, Washington **1996**.
[10] A. Caneschi, D. Gatteschi, L. Pardi, R. Sessoli, *Clusters, Chains and Layered Molecules: the Chemist's Way to Magnetic Materials*, in: A. F. Williams (Ed.), *Perspectives in Coordination Chemistry*, VCH, Weinheim **1992**.
[11] R. Cortés, L. Lezama, J. L. Pizarro, M. I. Arriortua, X. Solans, T. Rojo, *Angew. Chem. Int. Ed. Engl.* **1994**, *33*, 2488.
[12] G. Viau, M. G. Lombardi, G. D. Munno, M. Julve, F. Floret, J. Faus, A. Caneschi, M. J. Clemente-Juan, *J. Chem. Soc, Chem. Commun.* **1997**, 1195.
[13] F. A. Mautner, R. Cortés, L. Lezama, T. Rojo, *Angew. Chem. Int. Ed. Engl.* **1995**, *35*, 78.
[14] A. Escuer, R. Vicente, M. A. S. Goher, F. A. Mautner, *J. Chem. Soc., Dalton Trans.* **1997**, 4431.
[15] J. Ribas, M. Monfort, C. Diaz, C. Bastos and X. Solans, *Inorg. Chem.* **1994**, *33*, 484.
[16] R. Cortés, J. L. Pizarro, L. Lezama, M. I. Arriortua, T. Rojo, *Inorg. Chem.* **1994**, *33*, 2697.
[17] A. Escuer, R. Vicente, M. A. S. Goher, F. A. Mautner, *Inorg. Chem.* **1997**, *36*, 3440.
[18] R. Cortés, M. Drillon, X. Solans, L. Lezama, T. Rojo, *Inorg. Chem.* **1997**, *36*, 677.
[19] A. B. P. Lever, *Inorganic Electronic Spectroscopy*, Elsevier Science Publishers B.V., Amsterdam, Netherlands **1984**.
[20] J. Escobal, J. L. Mesa, J. L. Pizarro, L. Lezama, R. Olazcuaga, T. Rojo, *J. Mater. Chem.* **1999**, *9*, 2691.
[21] J. Escobal, J. L. Pizarro, J. L. Mesa, L. Lezama, R. Olazcuaga, M. I. Arriortua, T. Rojo, *Chem. Mater.* **2000**, *12*, 376.
[22] J. P. Hay, J. C. Thibeault, R. J. Hoffmann, *J. Am. Chem. Soc.* **1975**, *97*, 4884.
[23] C. Mealli, D. M. Proserpio, *Computer Aided Composition of Atomic Orbitals (CACAO)*. PC version, July **1992**, Kindly supplied by C. Mealli. See also: C. Mealli, D. M. Proserpio, *J. Chem. Edu.* **1990**, *67*, 399.
[24] L. F. Tang, L. Zhang, L. C. Li, P. Cheng, Z. H. Wang, J. T. Wang, *Inorg. Chem.* **1999**, *38*, 6326.
[25] M. A. M. Abu-Youssef, A. Escuer, D. Gatteschi, M. A. S. Goher, F. A. Mautner, R. Vicente, *Inorg. Chem.* **1999**, *38*, 5716.
[26] M. A. M. Abu-Youssef, A. Escuer, M. A. S. Goher, F. A. Mautner, R. Vicente, *Eur. J. Inorg. Chem.* **1999**, 687.
[27] A. Escuer, R. Vicente, M. A. S. Goher, F. Mautner, *Inorg. Chem.* **1998**, *37*, 782.
[28] A. C. T. North, D. C. Philips, F. S. Mathews, *Acta Crystallogr., Sect. A* **1968**, *24*, 351.
[29] A. Chandrasekaran, *XRAYACS*, Program for Single Crystal X-ray Data Corrections, Chemistry Department, University of Massachusetts, Amherst, USA **1998**.
[30] G. M. Sheldrick, *SHELXS 97*, Program for the Solution of Crystal Structures, University of Göttingen, Germany **1997**.
[31] G. M. Sheldrick, *SHELXL 97*, Program for the Refinement of Crystal Structures, University of Göttingen, Germany **1997**.
[32] *International Tables for X-ray Crystallography*, Kynoch Press, Birmingham, England, Vol. IV, p. 99, **1974**.
[33] C. K. Johnson, *ORTEP*, Report ORNL-5138, Oak Ridge National Laboratory, Oak Ridge, TN, **1976**.

Received October 18, 2000
[I00393]